LAPP Experimental Physics Seminar
February 2nd, 2010

Pair Production in light-by-light Scattering

Thomas Koffas

(CERN)

Overview

- Introduction and physics motivation
- Theoretical description
  - Electrons in strong external fields
  - Non-linear Compton scattering
  - Multi-photon pair production in light-by-light scattering
  - Spontaneous vacuum breakdown
- The electron beam
  - Beam preparation and steering
  - Electron beam focusing
- The laser system
  - Production of a high intensity laser pulse
  - Timing between the electron and laser beams
  - Establishing electron-laser beam collisions
- Detectors
- Data analysis
  - Positron signal reconstruction in the calorimeter
  - Measurement of the laser intensity parameters
  - Backgrounds and systematic effects
  - 46.6 GeV vs. 49.1 GeV data
- Results and comparison to theoretical models
- Conclusions

Physics Motivation

- QED has been tested extensively in the weak field regime:
  - Perturbative methods are applicable and theory agrees extremely well with the experiment
- In the case of strong fields perturbative techniques are of limited applicability
  - Processes can be treated within a semi-classical theoretical frame
  - Theory not tested against experimental measurements
- Strong fields are defined with reference to the QED critical field strength

$$\mathcal{E}_{crit} = m^2/e = 1.32 \times 10^{16}\ \text{V/cm} \quad (\hbar = c = 1)$$

- In fields of this strength various non-linear effects become prominent
- In this context the Breit-Wheeler process can be revisited
  - A multi-photon version of it could provide the necessary CM-energy to produce a e^+e^- pair
  - A two-step process in this approach using a laser induced external field:
    - A high energy electron scatters simultaneously off n laser photons, producing a high energy γ

$$n\omega + e^- \longrightarrow \gamma + e^-$$

    - The γ scatters again off n laser photons, while in the laser field, to produce a pair

$$n\omega + \gamma \longrightarrow e^+ + e^-$$

- This is the scheme employed by the E-144 experiment at SLAC
  - A table-top terawatt laser provided short pulses reaching a peak intensity of 10^{11} V/cm
  - At the rest frame of the 46.6 GeV electron beam it approaches the critical QED field strength
  - Pair production then becomes highly probable
- Results from this experimental effort will be presented here

Free Electron in an Intense Laser Beam

An electron in a circularly polarized wave (laser), executes a circular motion with radius

$r = \frac{e\mathcal{E}}{\gamma m\omega^2}$ or if define the parameter $\eta \equiv \gamma\beta_\perp = \frac{e\mathcal{E}}{m\omega} = \frac{p_\perp}{m}$, $r = \frac{\eta}{\sqrt{1+\eta^2}}\frac{\lambda}{2\pi} \leq \frac{\lambda}{2\pi}$

The parameter η is directly related to the laser intensity and consists a measure of it

$$\eta^2 = 3.65 \times 10^{-19} I\lambda^2 \quad \text{for } I \text{ in W/cm}^2 \text{ and } \lambda \text{ in } \mu\text{m}$$

where for convenience we have used: $\eta^2 = \frac{e^2\langle\mathcal{E}^2\rangle}{m^2\omega^2}$

The free electron appears to have an "increased" mass: $\bar{m} = m\sqrt{1+\eta^2}$

We can reach the same conclusions quantum mechanically starting from Dirac's equation

$$[\gamma(p - eA) - m]\psi = 0$$

that describes a free electron in a plane electromagnetic field with a 4-vector k^μ $(k^2 = 0)$:

Solving for plane wave solutions in the Lorentz gauge, one can find that the time average of the kinetic momentum operator $\boldsymbol{p - eA}$ to be: $q^\mu = p^\mu - \frac{e^2\langle A^2\rangle}{2(kp)}k^\mu$

Defining once more $\eta^2 = -e^2\langle A^2\rangle/m^2$ we find finally that: $q^\mu = p^\mu + \frac{\eta^2 m^2}{2(kp)}k^\mu$

Again the electron appears to have an effective mass ($q^2 = m_*^2$,): $\bar{m} = m\sqrt{1+\eta^2}$

Photon Emission by an Electron in a Strong Electromagnetic Field

The relevant quantity for the strength of the field is the parameter $\eta^2 = -e^2\langle A^2\rangle/m^2$

This can have arbitrarily large values and therefore perturbative techniques are not applicable. Still one can use the Born approximation for the calculation of the S-matrix elements where the strong electromagnetic field is treated classically since it is described by its 4-vector potential. Essentially in this case the electron is scattered off the field and not off a photon.

We can compute the cross sections in the case of both a circularly and a linearly polarized wave

$$A = a_1 \cos\phi + a_2 \sin\phi$$
$$a_1 = (0, a, 0, 0)$$
$$a_2 = (0, 0, a, 0)$$

Circular Polarization

where $\phi = (kx)$

$$A = a_1 \cos\phi$$
$$a_1 = (0, a, 0, 0)$$

Linear Polarization

The differential cross sections then describing the emission of a photon by an electron after absorbing n field photons are:

$$\frac{d\sigma_n}{du} = 2\pi r_0^2 \frac{m^2}{(s-m^2)}\frac{1}{\eta^2}\frac{1}{(1+u)^2}\left[-4J_n^2(z) + \eta^2\left(2+\frac{u^2}{(u+1)}\right)\left(J_{n+1}^2(z) + J_{n-1}^2(z) - 2J_n^2(z)\right)\right]$$

Circular Polarization

$$\frac{d\sigma_n}{du} = 2r_0^2 \frac{m^2}{(s-m^2)}\frac{1}{\eta^2}\int_0^{2\pi}\frac{d\phi}{(1+u)^2}\left[-2A_0^2 + 2\eta^2\left(2+\frac{u^2}{(1+u)}\right)\left(A_1^2 - A_0A_2\right)\right]$$

Linear Polarization

where $z = 2n\frac{\eta}{\sqrt{1+\eta^2}}\sqrt{\frac{u}{u_n}\left(1-\frac{u}{u_n}\right)}, \quad u_n = \frac{2n(kp)}{m^2}, \quad u = \frac{(kk')}{(kp')}$

Non-linear Compton Scattering

In the case of a weak plane wave field, i.e. when η is very small, one can expand the expressions before in powers of η. In the case of the circular polarization this results to:

$$\frac{d\sigma_n}{du} = 2\pi r_0^2 \frac{m^2}{(s-m^2)}\frac{1}{(1+u)^2}\left(\frac{1}{(n-1)!}\right)^2\left(n\sqrt{\frac{u}{u_n}\left(1-\frac{u}{u_n}\right)}\right)^{2n-2}\eta^{2n-2}\times \left[-4\frac{u}{u_n}\left(1-\frac{u}{u_n}\right)+2+\frac{u^2}{u+1}\right]$$

In the case of a single absorbed photon this becomes:

$$\frac{d\sigma_1}{du} = 2\pi r_0^2 \frac{m^2}{(s-m^2)}\frac{1}{(1+u)^2}\left[2+\frac{u^2}{1+u}-4\frac{u}{u_1}\left(1-\frac{u}{u_1}\right)\right]$$

and integrating we get:

$$\sigma_1 = 2\pi r_0^2 \frac{1}{u_1}\left[\left(1-\frac{4}{u_1}-\frac{8}{u_1^2}\right)\log(1+u_1)+\frac{1}{2}+\frac{8}{u_1}-\frac{1}{2(1+u_1)^2}\right]$$

which is the Klein-Nishina cross section for the Compton scattering

Essentially the cross sections for both the linear and the circular polarization describe the scattering of an electron off n field (laser) photons, i.e. the interaction

$$n\omega + e^- \longrightarrow \gamma + e^-$$

For the kinematic calculations we need to use the electron quasi-momentum as defined before and therefore momentum conservation gives:

$$nk^\mu + q^\mu = k'^\mu + q'^\mu$$

Non-linear Compton Scattering

Electron scattering off n laser(field) photons will constitute the n^{th} order Compton scattering the non-linear cases corresponding to n>1

The differential rates for the non-linear Compton scattering are then given by the expression

$$\frac{dN_n}{dE} = \frac{d\sigma_n}{dE} v_{rel} \int_{-\infty}^{+\infty} d\vec{x} \cdot dt \cdot \rho_e \cdot \rho_\omega$$

For small η's the differential rates are proportional to η^{2n}

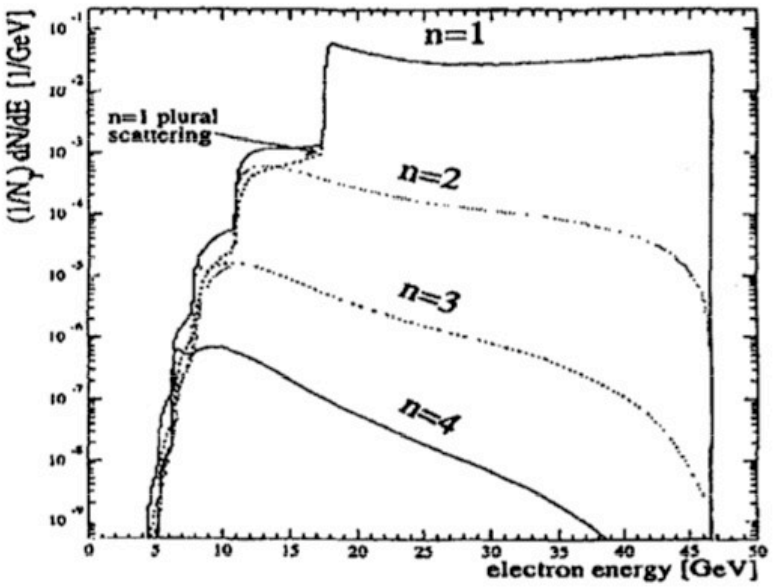

Electron spectra of various orders of Compton scattering. The γ spectra can be derived by subtracting the electron energies from the 46.6 GeV original electron beam energy.

Pair Production in Light-by-Light Scattering

Here the process is the production of a pair in light-by-light scattering where a high energy γ produced during the (non)-linear Compton scattering interacts with n laser photons

$$n\omega + \gamma \longrightarrow e^+ + e^-$$

The minimum energy for the γ required for the production of a pair is given by:

$$\omega_\gamma^{min} = \frac{2m^2(1+\eta^2)}{n\omega(1-\cos\alpha)}$$

And it's clearly a function of both the number of participating photons and of the laser intensity parameter η. Inversely for a specific γ energy, the minimum number of necessary laser photons can be derived. The largest pair production rates are achieved for 4 laser photons

Since the pair production is related by crossing symmetry to that of the Compton scattering the cross sections can be derived from the Compton ones

$$\frac{d\sigma_n}{du} = 4\pi r_0^2 \frac{m^2}{s}\frac{1}{\eta^2}\frac{1}{u\sqrt{u(u-1)}}\left[J_n^2(z) + \frac{\eta^2}{2}(2u-1)(J_{n+1}^2(z) + J_{n-1}^2(z) - 2J_n^2(z))\right]$$ Circular Polarization

$$\frac{d\sigma_n}{du} = 2r_0^2 \frac{m^2}{s}\frac{1}{\eta^2}\int_0^{2\pi}\frac{d\phi}{u\sqrt{u(u-1)}}\left[A_0^2 + 2\eta^2(2u-1)(A_1^2 - A_0A_2)\right]$$ Linear Polarization

where $z = \frac{2\eta}{u_1\sqrt{1+\eta^2}}\sqrt{u(u_n-u)}$, $u_1 = \frac{(kk_\gamma)}{2\bar{m}^2}$, $u_n = nu_1$, $u = \frac{(kk_\gamma)^2}{4(kq_-)(kq_+)}$

Pair Production in Light-by-Light Scattering

The differential cross sections are higher for the cases of fewer participating photons

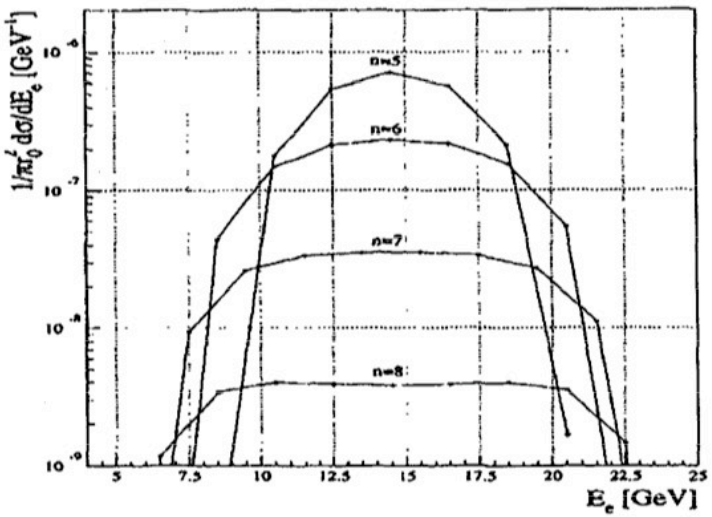

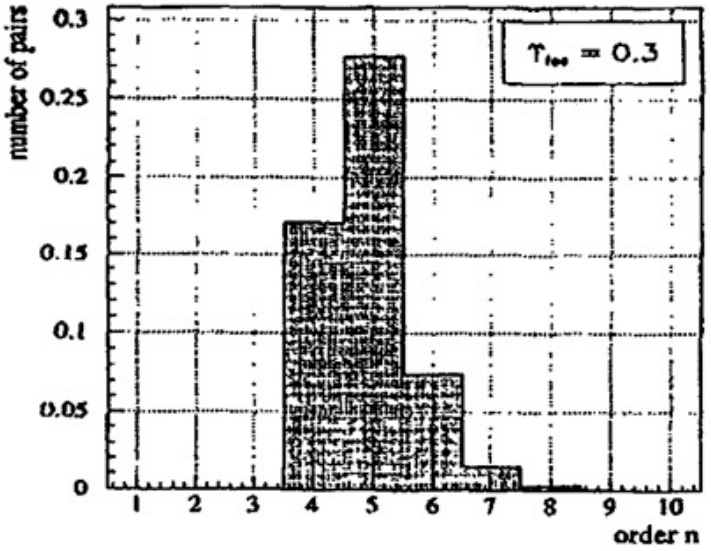

The highest pair production rates are achieved in the case of 5 participating photons, one of which being the high energy γ and the remaining 4 the low energy laser photons

For a complete treatment of the pair production the polarization of the initial high energy photon needs to be also taken into account. In the end the results are identical to the ones presented up to now, so we will refrain from going into the details.

Spontaneous Vacuum Breakdown

- The quantum field ground state is characterized by "quantum" fluctuations during which short lived virtual e^+e^- pairs are created and then annihilated again
- In the presence of a strong external field the vacuum can become unstable
- Short-lived e^+e^- pairs can then become physically separated and transformed into real particles at the expense of some energy provided by the external field
- For this to happen the work done by such a field over the distance of one electron Compton length should be the mass of the e^+e^- pair and the external field should then have the strength of the QED critical field

In a purely static external field pair production can be described in terms of quantum mechanic tunneling of a positron from the Dirac sea through the classically forbidden zone under the influence of an external potential energy. Then the probability is

$$P \sim \exp\left(-2\int_{x_-}^{x_+}\sqrt{m^2-(e\mathcal{E}x)^2}dx\right) = \exp\left(-2\int_{x_-}^{x_+} q(x)dx\right)$$

$$P \sim \exp\left(-\frac{2m^2}{e\mathcal{E}}\int_{-1}^{+1}\sqrt{1-y^2}dy\right) = \exp\left(-\frac{\pi m^2}{e\mathcal{E}}\right) = \exp\left(-\frac{\pi}{\Upsilon}\right)$$

where we have defined the parameter $\Upsilon = \frac{e\mathcal{E}^*}{m^2}$

This is the probability of producing one pair. A more careful calculation yields

$$P = \frac{\alpha\mathcal{E}^2}{\pi^2}\sum_{n=1}^{+\infty}\frac{1}{n^2}\exp\left(-\frac{n\pi}{\Upsilon}\right)$$ for producing 1,2,…,n pairs

Spontaneous Vacuum Breakdown

- Pair production can also occur in the case of an alternating external field such as a laser field
- The individual photon energy needs to be much smaller than the electron mass
  - This is clearly satisfied in the case of normal laser wavelength
- Only the probability for producing a single pair is significant under these conditions

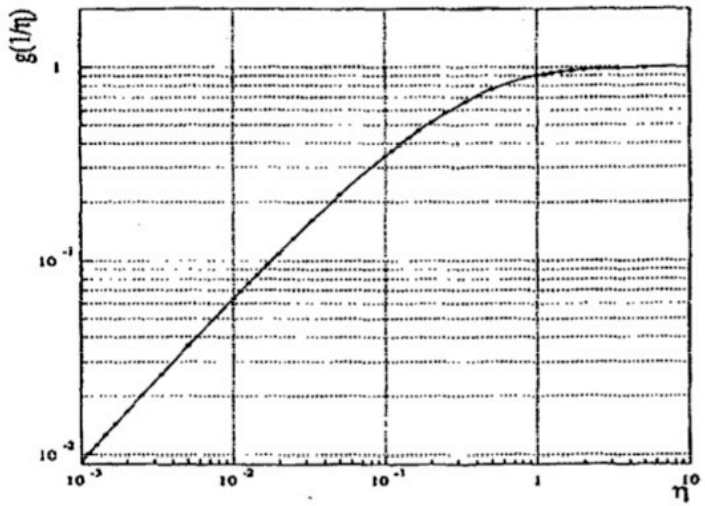

$$P = \frac{\alpha \mathcal{E}^2}{\pi} \frac{1}{g(z) + \frac{1}{2} z g'(z)} \exp\left(-\frac{\pi}{\Upsilon} g(z)\right)$$

where $$g(z) = \frac{4}{\pi} \int_0^1 dx \left(\frac{1 - x^2}{1 + x^2 z^2}\right)^{1/2}, \quad z = 1/\eta$$

At the high frequency limit: $$P \simeq \frac{\alpha \mathcal{E}^2}{\pi} \exp\left(-\frac{\pi}{\Upsilon}\right), \quad \eta \gg 1$$ (tunneling result)

At the low frequency limit: $$P \simeq \frac{\alpha \mathcal{E}^2}{8} \left(\frac{e\mathcal{E}}{2m\omega}\right)^{4m/\omega}, \quad \eta \ll 1$$

where the exponent can be interpreted as the minimum number of laser photons required to produce a pair

The Electron Beam

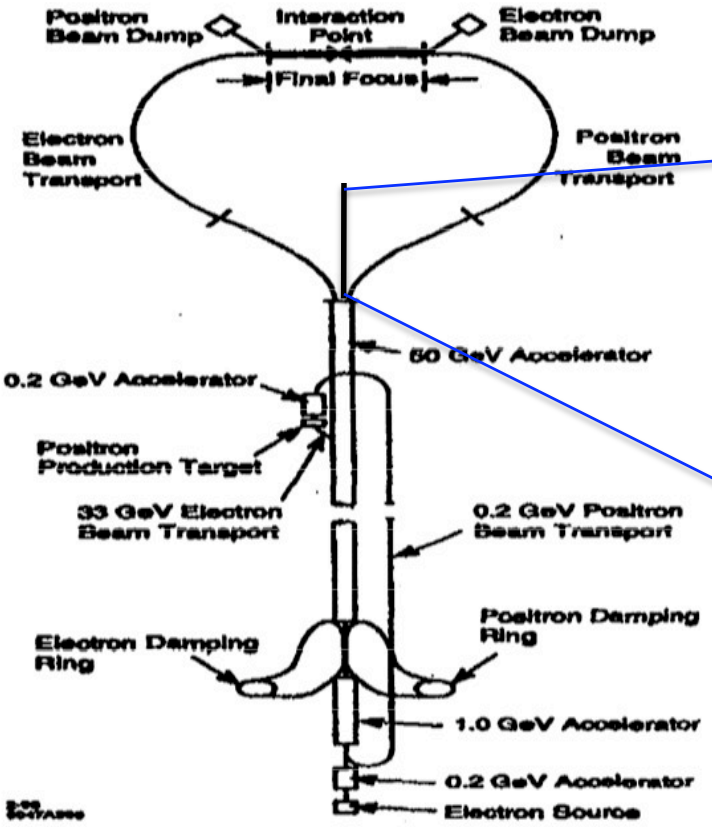

FFTB Line

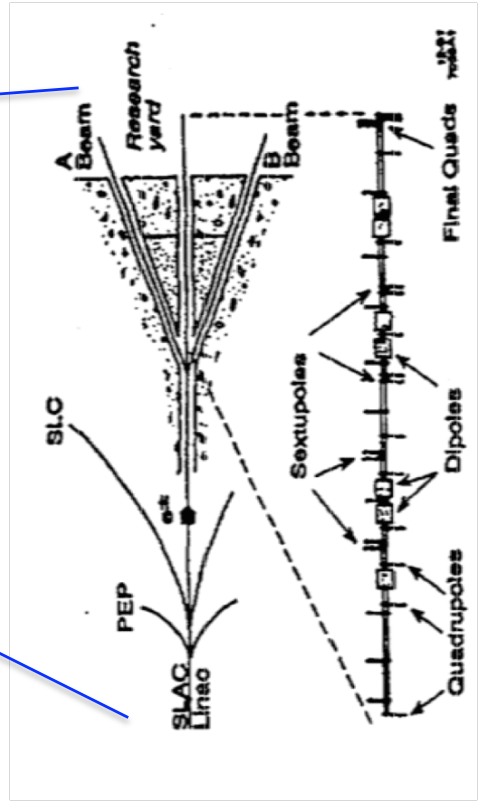

- The experiment was installed in the FFTB line:
  - Located at the end of the 2-mile long linac
  - Line designed for focusing electron beams to sub-μm levels
  - No acceleration involved, pure beam optics line
  - Small focal areas increase the number of e^- through the laser beam and hence event rates
- Bunch lengths of <1 mm and beam charges of $5\text{-}7\times10^{9}$ have been delivered
- Normalized emittance of 3×10^{-5},3×10^{-6} in x,y transverse dimensions respectively
  - A measure of the electron beam size and divergence delivered at the FFTB line

The FFTB Line

- The beta-match line
  - Contains quadrupole magnets to match the incoming beam parameters to those desired at the focus
- The chromaticity correction lines
  - Focal spot sizes increase with increased energy spread of the beam (chromaticity)
  - The chromaticity correction lines minimize the energy spread by employing sextupole magnets
  - Correction needs to be performed separately for the two transverse dimensions (x,y)
    - Require $\beta_x >> \beta_y$ to correct for the horizontal chromaticity and the opposite for the vertical one
    - A line in between the two chromaticity correction lines called the Beta Exchanger achieves that
- The final telescope line
  - Contains quadrupole magnets for the final electron beam focusing
  - Smaller sextupole magnets are used for correcting residual aberrations from all previous lines
- The dump line
  - Used to steer the beam to the dump
  - The electron-laser beam interaction point (IP) is located here 12.5 m downstream the FFTB final focus
- The incoming to the FFTB electron beam position and angular jitter need to be controlled
  - This decouples the FFTB line steering from all the effects upstream in the linac
  - An active feedback using BPMs (reference) and correctors in front of the FFTB is employed
  - Resulting stability in position is ~1 μm and in angle ~0.016 μrad
- Similar control is necessary for the incoming electron beam energy jitter
  - A feedback system using BPMs at the FFTB dump line and klystrons in the linac is employed
  - The resultant energy jitter measured at the dump line is 7 MeV for the 46.6 GeV electron beam
- A collimation scheme to remove e^- with large excursions in energy, position, angle is used

Electron Beam Spot Size Tuning at the IP

- The incoming to the FFTB beam parameters are measured and matched to the FFTB design
  - This is the Beta Matching procedure employing the magnets in the FFTB Beta Match line.
- A beam waist is then established at the FFTB final focus point
- The waist is then transferred 12.5 m downstream at the IP using the dump line quadrupoles
  - Beam divergences that result in high background levels in PCAL need to be minimized
- Beam size is measured in two ways:
  - Moving a set of wires placed at the IP across the electron beam
  - Scanning the electron beam across the stationary wires at the IP using dither correctors upstream

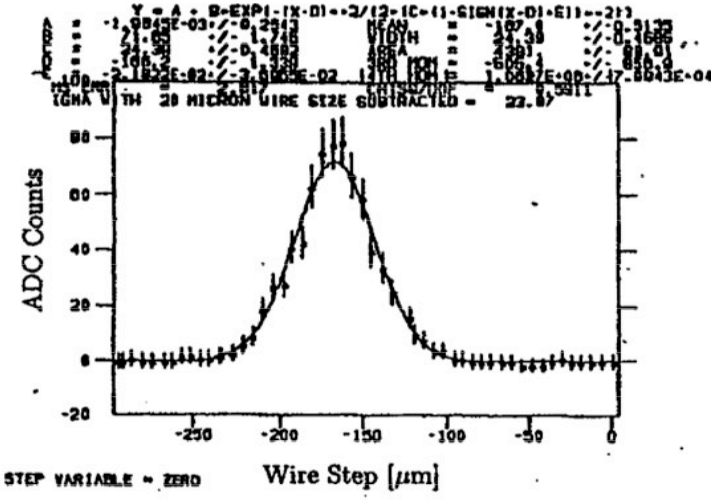

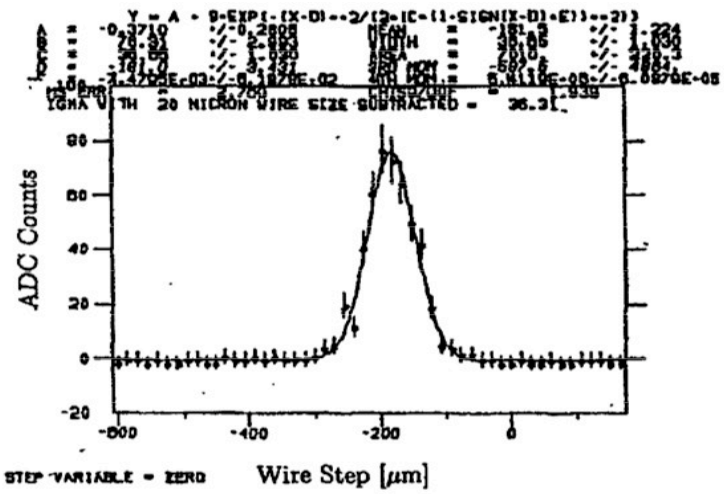

- Spot sizes of 21×37 μm in x,y respectively for the 46.6 GeV beam have been measured
  - The small distance between the FFTB final focus and the E-144 IP results in much larger sizes there
- Energy, position and angle feedbacks like those used by the FFTB are turned on after steering
- Similar procedure followed for the 49.1 GeV electron beam, giving 32×32 μm spot sizes
  - Electron energy limited by the permanent bending magnets at the FFTB dump line
  - Requires scaling of the FFTB magnets by a factor of 49.1/46.6, together with the linac klystrons

Laser System

- The laser is a Table Top Terawatt (T^3) solid state system, that operates at 0.5 Hz
- Delivers both IR (1054 nm) and Green (527nm) pulse
- The polarization is chosen to be either linear or circular using a liquid crystal polarizer
- Maximum energies of 2J (for the IR) and 1J (for the green) have been delivered at the IP
- Focal points were 2 and 4.7 times the diffraction limited ones for the IR and green pulses.
- The pulse time widths are 1.5 ps for both wavelengths
- Intensities above 10^{18} W/cm^2 have been achieved at the focal point

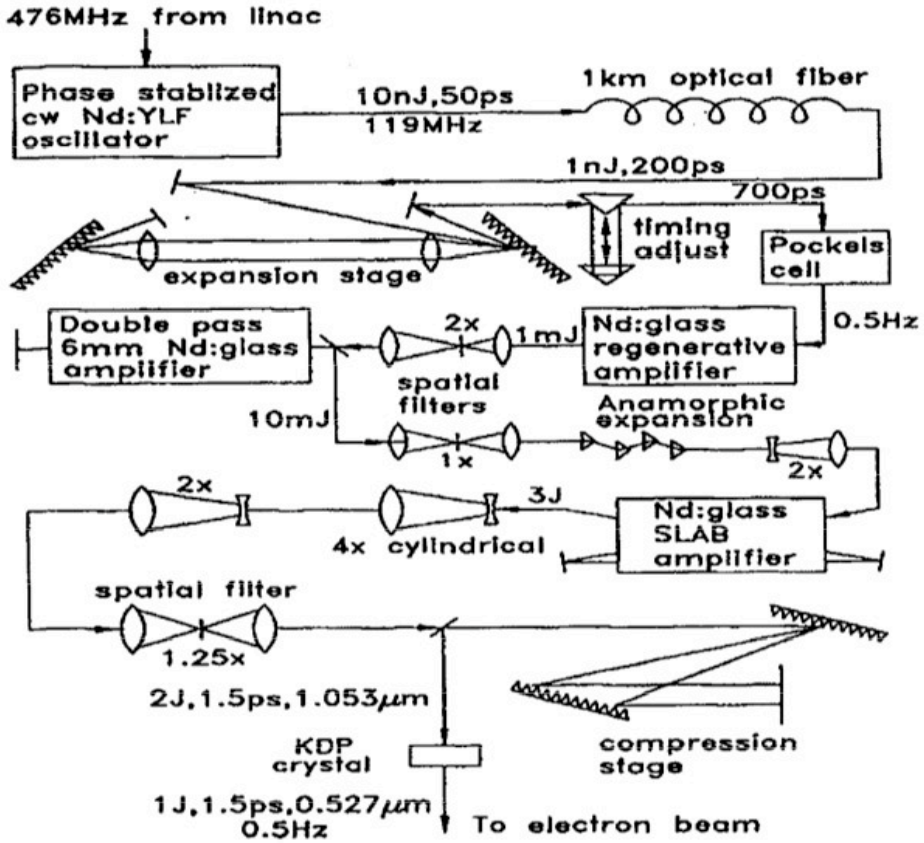

It consists of:

- An Nd:YLF modelocked oscillator
- An Nd:Glass regenerative amplifier (regen)
- A two-pass Nd:Glass rod amplifier
- A three-pass Nd:Glass slab amplifier

The Laser Oscillator

- A Nd:YLF flash-lamp pumped mode-locked cavity
- The modelocker is driven by the linac RF (476 MHz) frequency divided by 8 (59.5 MHz)
- A cooling system to keep the modelocker temperature stable at ~30 ^{0}C is employed
- A phase locked feedback loop maintains the phase of the laser pulses to the reference RF
- The oscillator produces a 119 MHz, 50 ps pulse train at 1054 nm (IR)
- The pulse train goes through 1 km long optical fiber where two effects take place:
  - Time stretching due to Group Velocity Dispersion
  - Frequency chirping due to Self Phase Modulation
- The diagnostics line consists of:
  - A spectrometer to measure the bandwidth (32 angstroms) around the 1054 nm wavelength
  - A cw autocorrelator to measure the pulse width (1.5 ps)

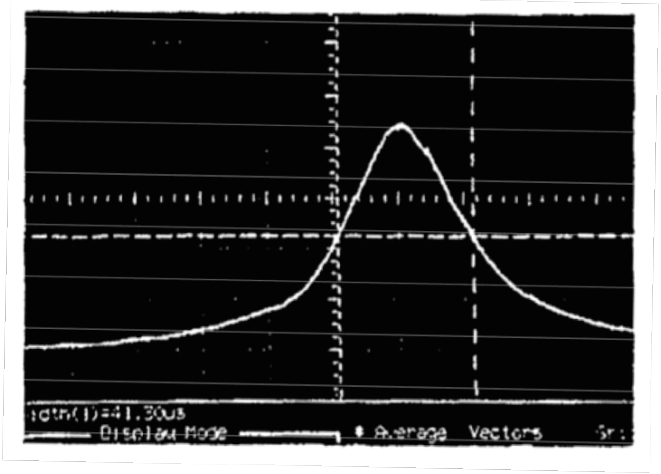

- An expansion grating further expands the pulses in time to ~700 ps
  - Expansion in the frequency domain allows for further compression in time later

Laser Energy Amplification

- At the exit of the oscillator the energy energy is 1nJ and the pulse width 700ps
- Every 2s a pulse out of the oscillator pulse train is selected and further amplified in energy
- There are three amplification stages:
  - A Q-switched Nd:Glass regenerative amplifier (regen) that produces a 1mJ pulse
  - A 2-pass Nd:Glass rod amplifier that results in a 10mJ pulse
  - A 3-pass Nd:Glass slab amplifier that produces up to 2J pulses
- After every amplification stage a telescope cleans the pulses from any intensity variations

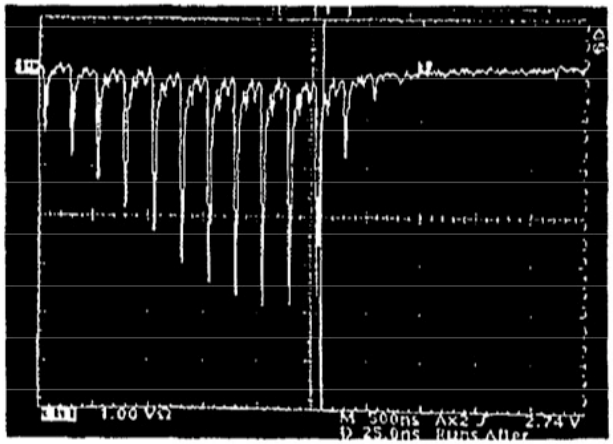

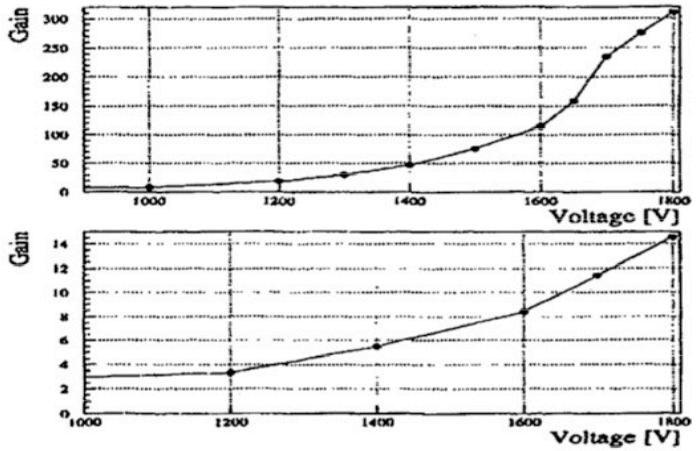

- The repetition rate is defined by the cooling requirements of the amplification stages
  - If not enough cooling time is allowed distortions to the pulse wavefront are induced
  - This results in sub-optimal laser pulse focusing and time compression
- After the slab amplifier the laser pulse is re-circularized using cylindrical lenses
- A waveplate selects the pulse polarization (either circular or linear)
- The laser pulse spot size is also increased to improve the focus quality later
- The laser pulse eventually is also compressed in time to ~1.5ps widths

Laser Transport & Interaction Point

- The laser pulses are transported by a 12 m periscope at high vacuum to the IP
- The pulse is focused by an Off Axis Paraboloid (OAP) on the electron beam
- It is then re-collimated by another OAP and returned to the laser room for diagnostics

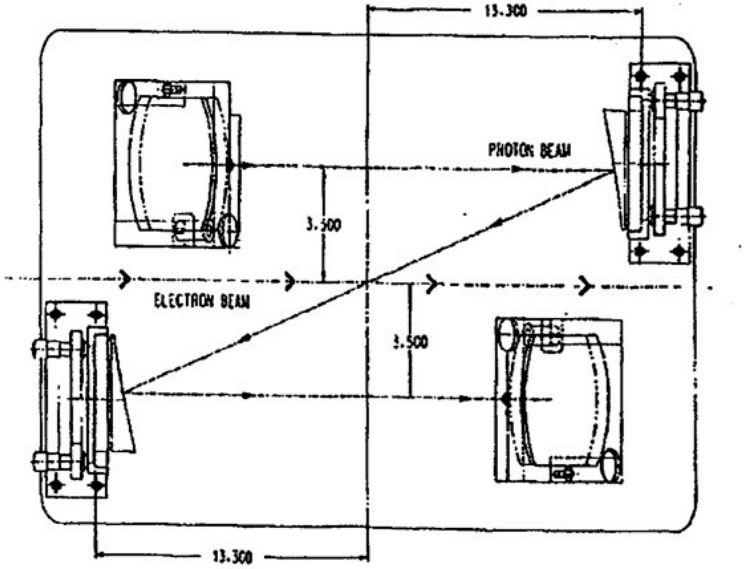

IP design. The laser crosses the electron beam at 17^0. All the optics are mounted on an invar plate to reduce thermal effects.

- The OAP alignment is critical for the optimal laser focusing of the laser pulse
  - A Mach-Zehnder interferometer was used together with a He-Ne beam that traverses all the IP optics
  - The deflecting mirrors were placed on micro-rotators for the final alignment tuning
  - An active feedback for long-term misalignements was also in place

Laser-Electron Beam Timing

- This is the most important technical challenge in the experiment requiring ps precision
  - It ensures the timing of a 7 ps electron bunch to a 1.5 ps laser pulse
- A sub-multiple of the master accelerator frequency (476 MHz) drives the laser oscillator
- This sets the time of the laser pulse launching
- An electronic feedback locks the phase of the oscillator to the accelerator RF
- Fine tuning is achieved by modulating the length of the laser beam path
  - Use an optical delay line (prism) to change the path length
  - Monitor the collision products using both the linear and non-linear monitors

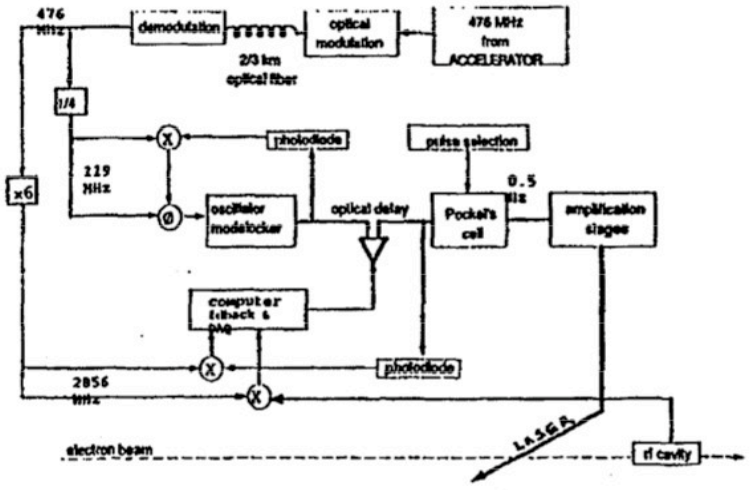

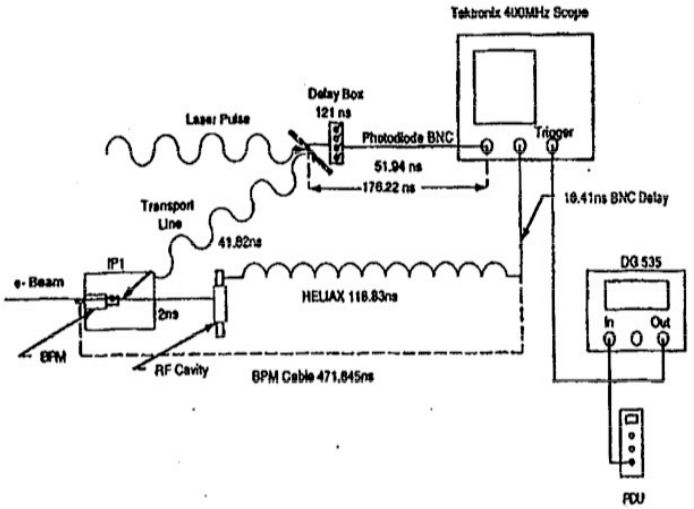

- The laser timing is set by the switch-out time of the regen (trigger synchronized to the linac RF)
- A photodiode in the transport line, collects light leakage and provides the laser time reference
- This is compared to an electron beam based signal provided by a ringing cavity
- Coarse timing (~0.5 ns) is established using a Pulse Delay Unit (PDU)
- The optical delay line provides the remaining fine tuning down to ps precision

Timing Jitter and Long Term Drift

- The timing jitter can be deduced by direct phase comparison of the pulse train and the linac RF
- Use a Double Balanced Mixer and perform the phase comparison at 2856 MHz
- The mixer DC output is proportional to the phase difference between the two inputs
- Using the mixer's calibration one can translate the DC voltage to time jitter

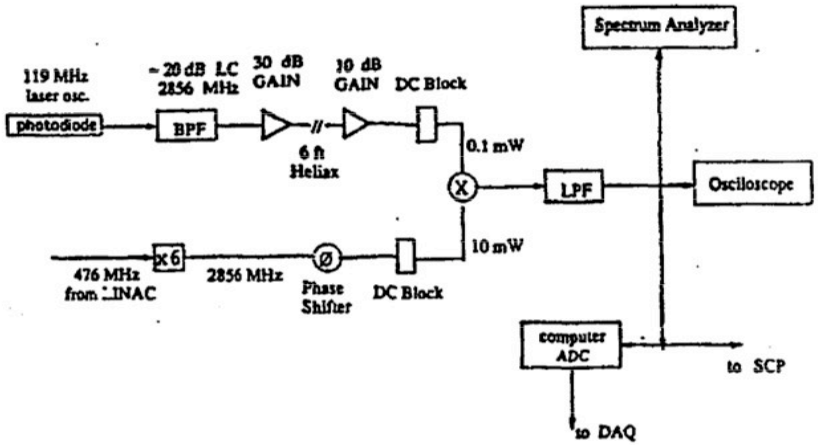

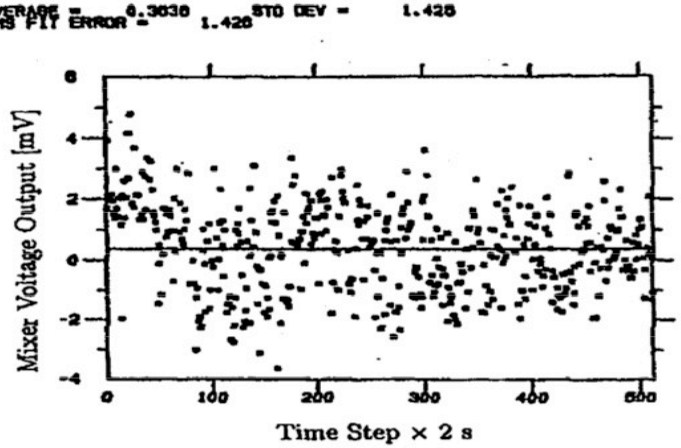

Jitter 1.4 ps

- Main source of timing jitter is the temperature variation of the oscillator modelocker

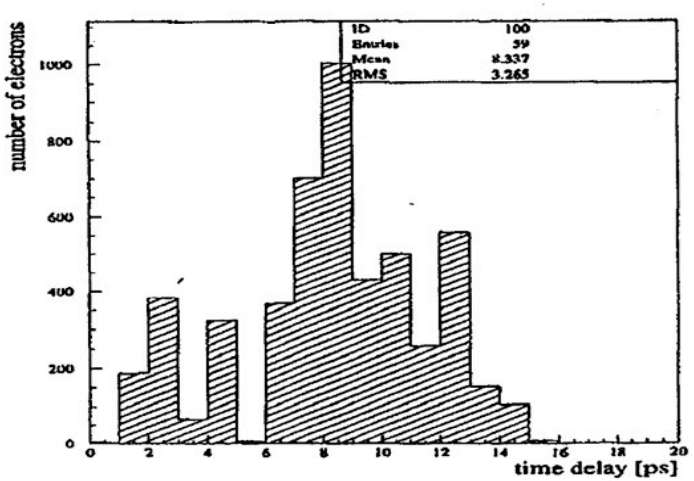

- Same method used for long term drift measurements
- Main source diurnal thermal effects (day-night variation)
- A timing drift of 6 ps/hr has been measured
- Can be corrected with timing scans
  - Modulate laser optical path
  - Measure collision products using the electron monitors

Laser Electron Beam Spatial Overlap

- A device (IP Flag) is placed at the focus of a He-Ne beam that coincides with that of the laser
- The electron beam is steered on the wire cross-hair using dither correctors
  - Use the γ monitors to establish optimal overlap (due to bremsstrahlung effects)
  - The alignment needs to be repeated every time the electron beam optics are modified
  - Due to thermal effects, long term drifts will appear
  - Perform X, Y- scans by moving the IP region (essentially laser focus) with respect to electron beam
    - Look at non-linear monitors for maximum signal
    - Requires optimal timing synchronization in advance

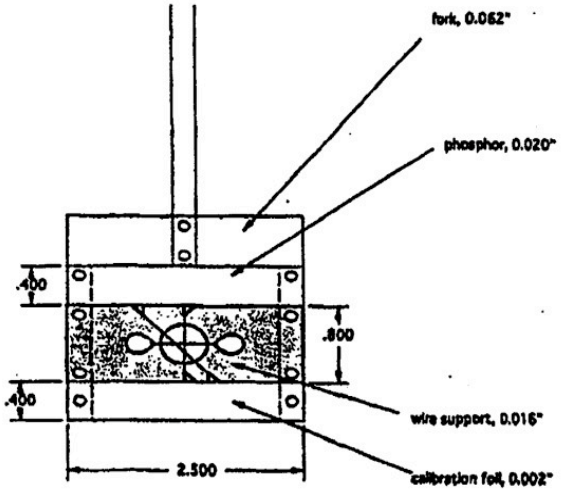

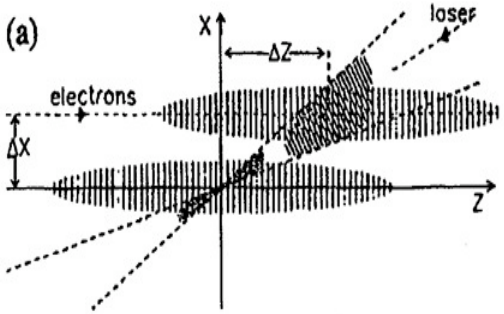

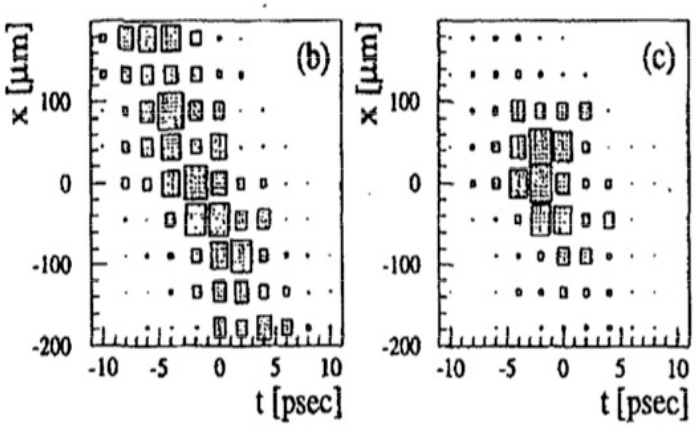

- There is a strong correlation between the x-position and the time overlap of the two beams
- Both can be optimized by performing an XT-scan and look at the non-linear monitor response
- Main drawback is that the XT-scan is time consuming

Calorimeters

- Two calorimeters are used to measure the energy of the charged particles, one for electrons (ECAL) and one for positrons (PCAL)
- Both calorimeters are of similar design:
  - Made of alternating layers of Si(300 μm thick) and Tungsten (1 X0 thick)
  - Each is divided in 12 rows and 4 columns resulting in 1.6×1.6 cm^2 pads
  - Groups of 4 rows per column make a tower; longitudinal layers per tower are arranged in segments

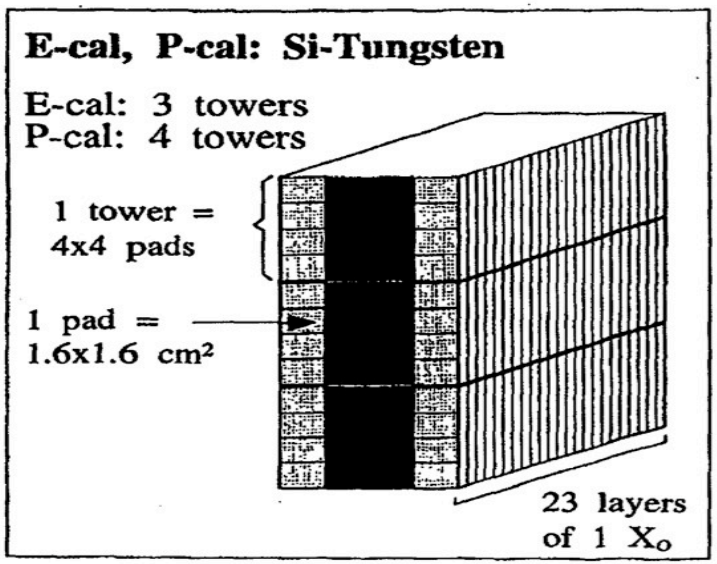

- Only the middle columns record signal, the outer columns used for background subtraction
- Gain in ECAL is set so that a 10GeV e^- can be detected, whereas a 10TeV e^- saturates it
- Gain in PCAL is 30 times higher, due to much lower background levels
- Calibration is done using e^- beams of variable yet known momenta
- The calorimeter resolution is measured to be:

$$\sigma_\varepsilon^2 = (0.19)^2\mathcal{E} + (0.4)^2 + (0.05)^2\mathcal{E}^2$$

Momentum map and calorimeter acceptance

- Downstream of the IP there is a spectrometer:
  - It consists of 6 permanent 4.48 kGauss bending magnets
  - Air core “soft” bending magnets (variable strength), are used to reduce synchrotron radiation
  - Electrons are bent downwards and positrons are bent upwards

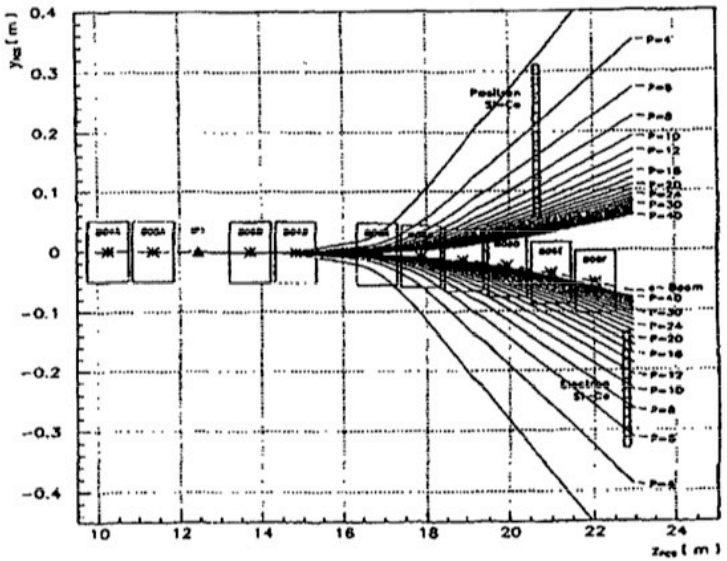

- A tracking algorithm maps the impact point of charged particles on the calorimeter:
  - Measured magnet field maps and locations are used as input
- Using the momentum map the acceptances of the two calorimeters can be determined:
  - ECAL moves vertically which results in increased acceptance, 6-11 GeV for a 46.6 GeV e^- beam
  - PCAL has a fixed position resulting in 6.8-21.5 GeV acceptance for a 46.6 GeV e^- beam
  - Both acceptances are shifted upwards by ~10% for a 49.1 GeV electron beam

Linear monitors

- Linear monitors are detectors looking at the linear Compton scattering signal
- Two types of linear monitors are used:
  - 1 air Cherenkov counter that intercepts γ's from the linear Compton scattering (CCM1)
  - 2 air Cherenkov counters that look at linear Compton scattered e^- of 37 and 31 GeV (EC37, EC31)

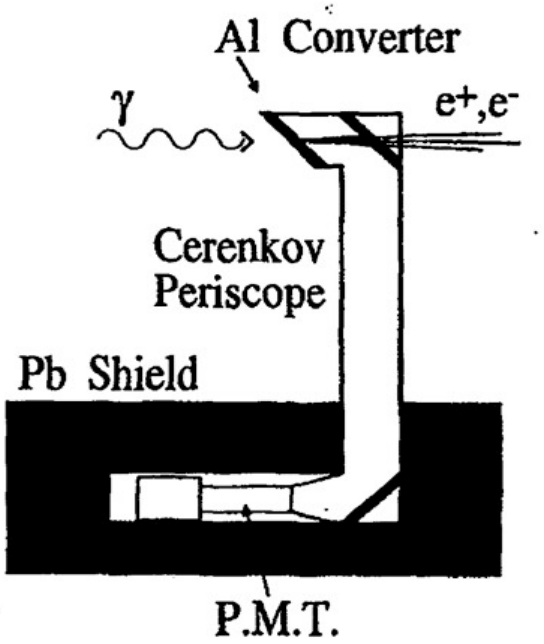

- Calibrate the CCM1 monitor using bremsstrahlung electrons from an Al foil
- Cross-calibrate the EC37, EC31 counters with respect to the CCM1 counter
- Linear monitor signal used in data analysis (N1) the average of the EC31, EC37 signals

Non-linear monitors

- They are also gas Cherenkov counters, using ethylene instead of air
- Two monitors exist, N2 , N3 intercepting 2nd and 3rd order Compton e- respectively

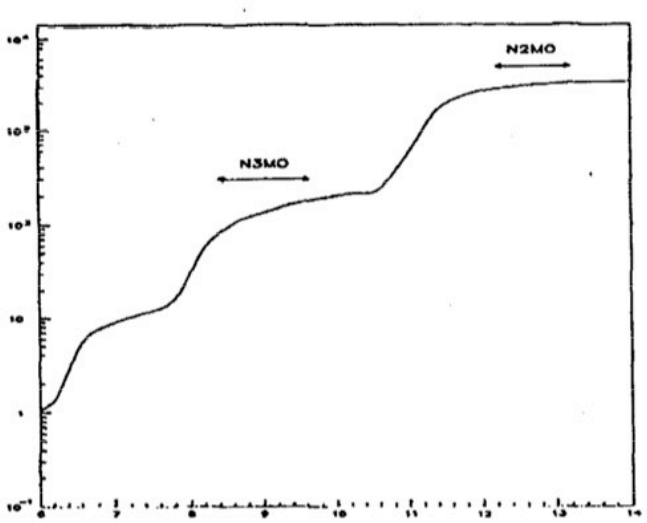

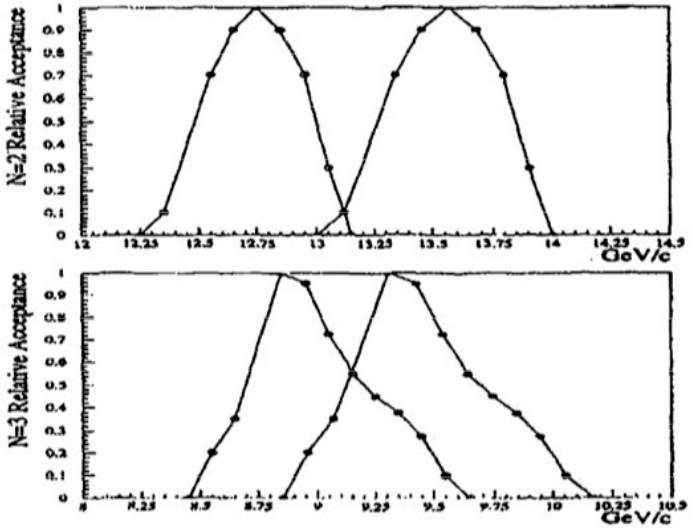

- The two monitors are cross-calibrated using ECAL and a test e- beam of variable momentum
  - Use the ECAL recorded signal to transform measured ADC counts into electrons
  - Using the high voltage settings in order to estimate the gain
  - The final number is corrected by folding in the expected non-linear Compton spectrum acceptance
- Different acceptances are found for the 46.6 and the 49.1 GeV electron beams:
  - The spectrometer settings downstream of the IP are different for the 46.6 and 49.1 GeV beams

Pair production in multiphoton light-by-light scattering 46.6 GeV electron beam data analysis

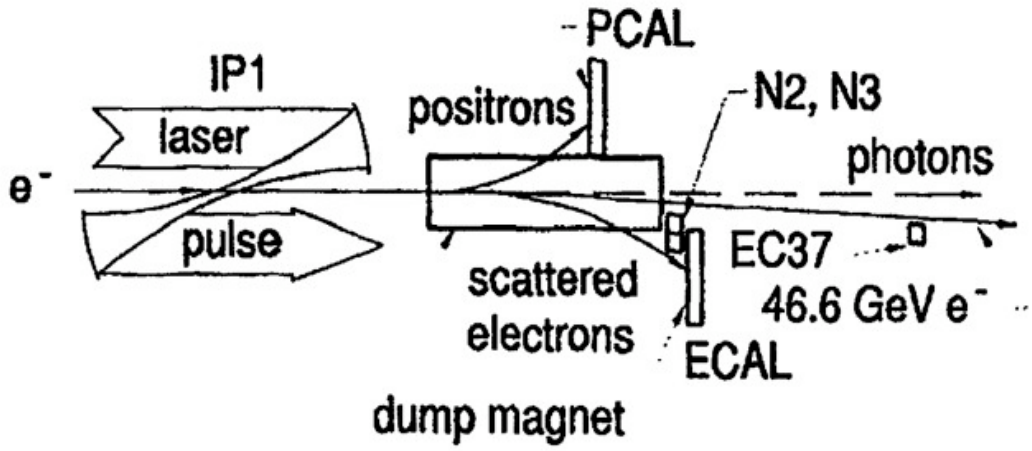

- A two-step process:
  - An energetic γ is produced by Compton scattering of 46.6 GeV e^- off n laser photons
  - While in the laser focus the γ absorbs n(=4) laser photons to produce a pair
- Produced charged particles are deflected towards the calorimeters:
  - e^+ are deflected towards PCAL
    - Due to the rarity of the process all backgrounds need to be kept low in PCAL
  - e^- are deflected towards the ECAL
    - They are swamped by the Compton scattered electrons; signal impossible to extract
- PCAL the primary detector for the pair production
- Signal should be optimal when:
  - Laser intensity (described by η) highest
  - Laser-electron beam spatial/temporal overlap optimal

Reconstruction of e^+ clusters in Si calorimeter

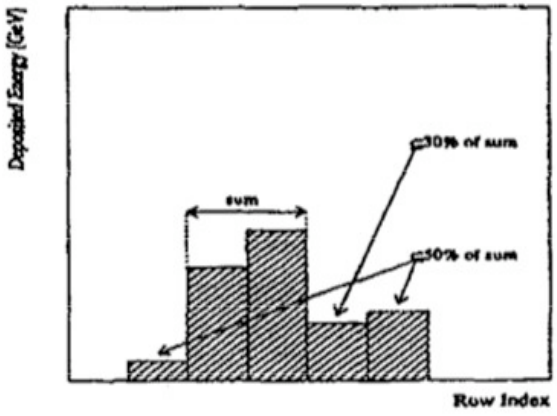

Cluster search algorithm:

- Row with highest deposited energy is determined
- Determine 5-row range by including 2 neighboring rows on each side
- Add energy of the two rows with the highest deposited energy
- Other adjacent row should contain <30% of energy in previous step
- Rest of rows should contain <50% of energy computed in step 3.
- Spatial extend of cluster defined by using the 3 central rows
- The e^+ energy is defined as the some of the energy in these 3 rows

Determination of cluster (x,y) position:

- Take log of energies in two hotest rows, i.e $\ln(E_2/E_1)$
- Shift cluster y-position from center of peak row accordingly
- If $E_2/E_1 < 0.15\ E_1$, then use $\ln(E_2/E_3)$
- If $E_2/E_3 < 0.07\ E_2$, then cluster y-position middle of peak row
- Use the cluster y-position to determine e^+ momentum
- Similar for cluster x-position

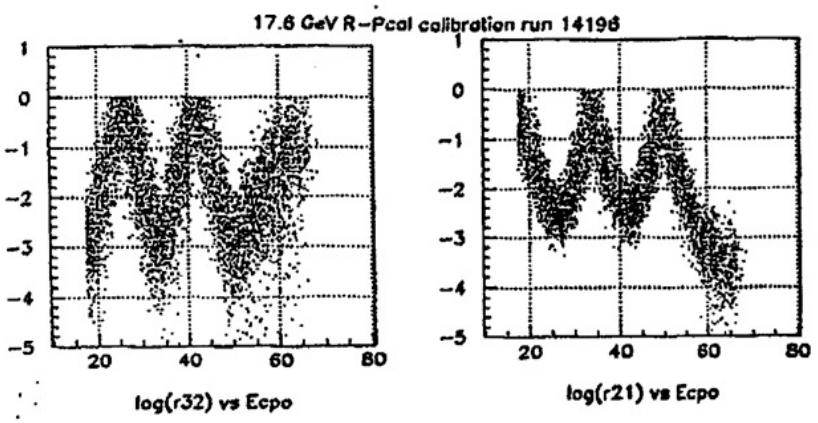

Use fixed momentum e^+ (17.6 GeV) to determine the ratio of energies vs. the PCAL position

Cluster search algorithm independent of original electron beam energy

Selection of e^+ clusters in Si calorimeter

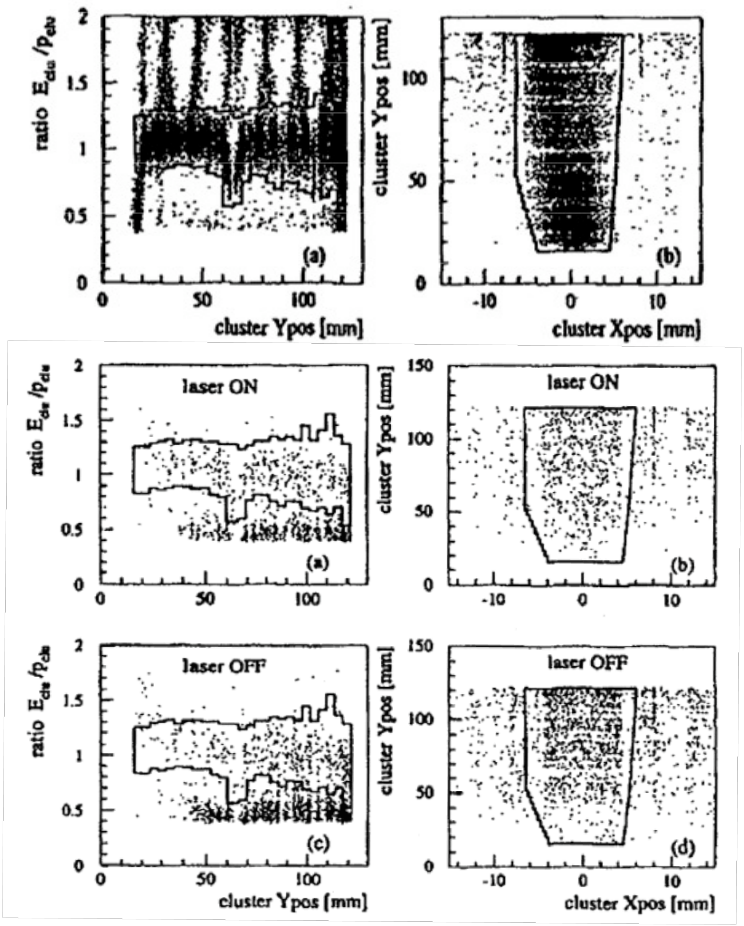

Statistical significance independent of cut tuning

⬇

Positron signal real

- Keep clusters where $E_{clus}/p_{clus} \cong 1$;
- Due to energy leakages ratio exhibits Gaussian distribution
- Use calibration data to select appropriate range:
  - Produce positrons via bremsstrahlung in a wire placed at the IP
- Range wider at higher cluster x,y-positions
  - Calorimeter resolution worse for softer positrons
- Selection needs to be position depended.
- Tune range around $E_{clus}/p_{clus} \cong 1$ to optimize:
  - The signal to noise ratio
  - Observed number of positrons
  - Statistical significance
- In addition optimize for laser-electron beam overlap conditions
  - Use ratio of measured n=1 Compton scatters over expectation
  - Optimize by looking at above 3 quantities

Positron signal after all cuts: 106 ± 14 e^+

46.6 GeV Data Results						
Cut Type	Laser ON	Laser OFF	Trig. Ratio ON/OFF	Sig/Noise	Ne^+	Statistical Significance
Optimal Cuts	21962	121216	0.1812	2.55±0.23	106±14	7.7σ
Loose Cuts	30810	121216	0.2542	2.10±0.17	118±16	7.4σ
Medium Cuts	21962	121216	0.1812	2.73±0.28	93±12	7.4σ
Tight Cuts	17189	121216	0.1418	4.05±0.53	70±10	7.2σ

Estimate of the laser intensity parameter η

- Laser intensity η a unique function of laser parameters (energy, pulse width, focal area)
  - Laser energy measured at best to within 10%
  - Laser focal area at interaction point of limited accuracy
  - Laser pulse width at interaction point not very reliable

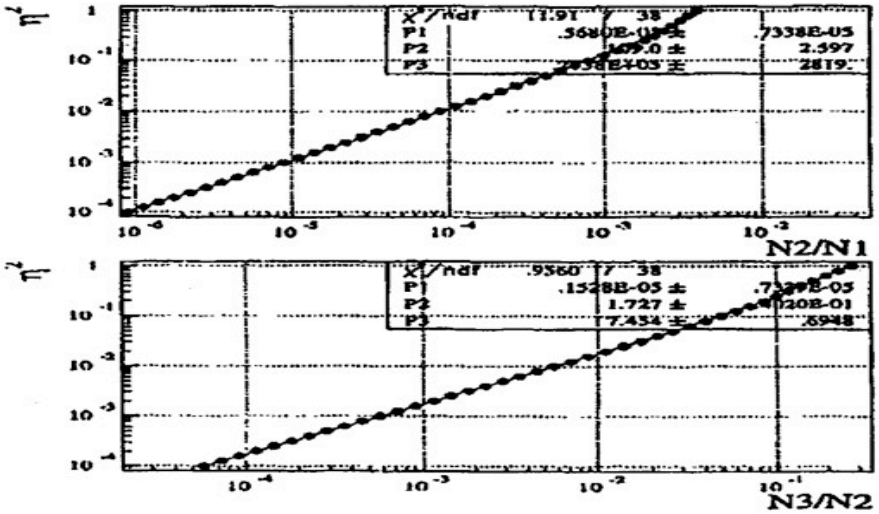

- But η^2 a function of the number of observed Compton scattered electrons of various orders:
  - $\eta^2 = k_1 (N_2/N_1)$ or $\eta^2 = k_2 (N_3/N_2)$
  - N_1, N_2, N_3, number of electrons measured by the 1^{st},2^{nd},3^{rd} order Compton scattering monitors
  - k_1 and k_2 depend on monitor efficiencies and acceptances
- η can be provided by any of the two relations; value consistent with the one from the other
  - Introduce a χ^2 fit method with the above constraint
  - No special assumption about the distribution of errors is necessary
- Constrained fit provides new values for N_1, N_2, N_3 along with new covariance matrix
  - Use any of the relations above to determine η afterwards

Use of the constrained fit to introduce a probability cut

- The distribution of the N3 monitor ADC counts not optimal, indicating a performance problem
- This will affect the constrained fit performance as well.
- Using simulated data, this leads to abnormally many low probability fit results
  - For uncorrelated input data to the fit, the probability distribution ought to be flat
- A correlation between the low probability peak and the long tail in the N3 ADC counts exists

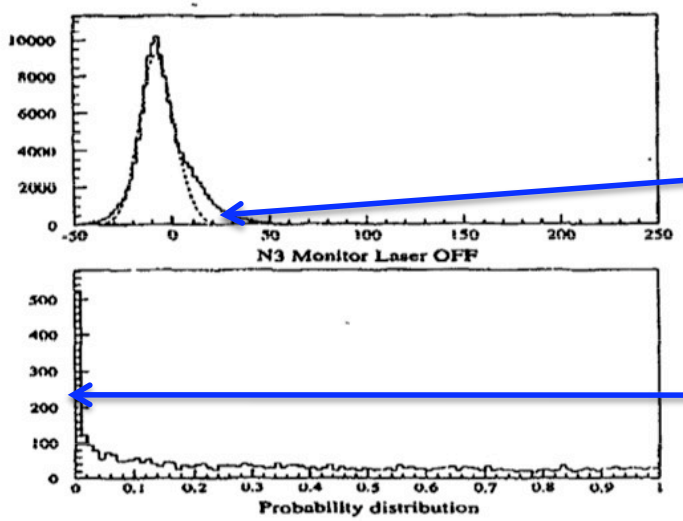

Long tail in N3 monitor ADC counts

Results in peak at low probabilities after the constrained fit

- Effect is clearly reproduced by data
- Can be ascribed to the N3 monitor problem
- Can be remedied by cutting the low probability peak

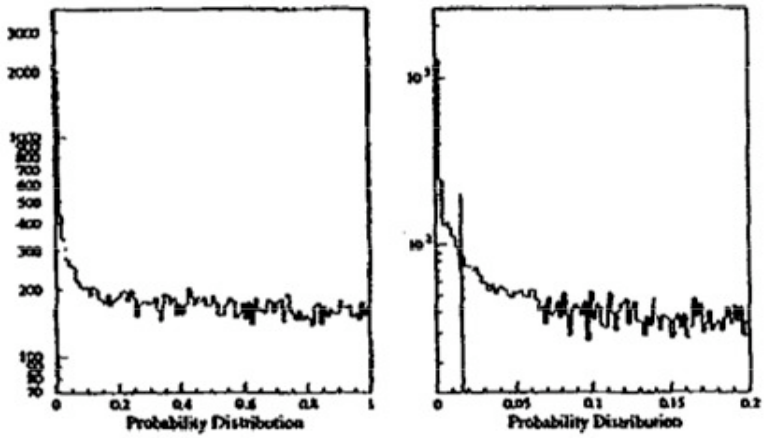

Scaling of the input signal of the three monitors

- Due to calibration problems the N1, N2, N3 monitor signals are significantly overestimated
  - This results to unacceptably high χ^2 fit values and event-by-event convergence problems
- To remedy that all three monitor signals need to be scaled down:
  - Plot the ratio of the measured over the predicted (from simulation) monitor signal
  - Select the scaling factor by choosing the ratio that contains 90% of the measurements

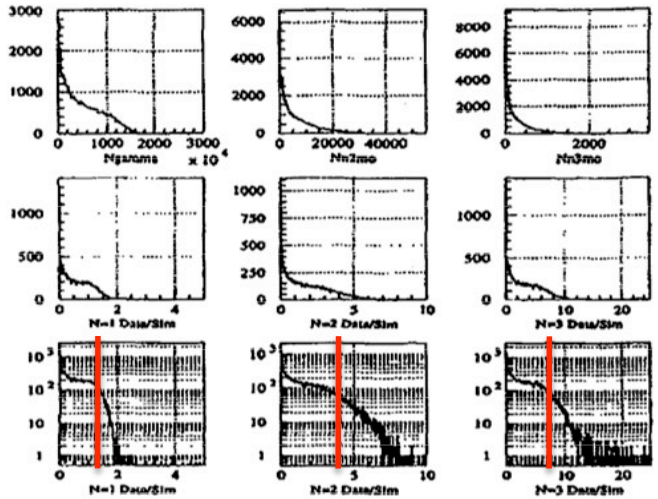

Plots that show the ratio of the measured over the predicted monitor signal. The red lines indicate the value where 90% of the signal is contained

- In addition scale upwards the N2 monitor error:
  - This in fact brings it to about the same value as the other non-linear monitor N3
- Different scaling factors result in different η's which is one input parameter to the simulation
  - 10% variation in the value of η, changes the simulation prediction by half order of magnitude
- Need iterative procedure to determine the final scaling factors and convergence in η value
  - Vary the scaling factors; estimate η; stop when relative difference in η small
- Use the η determined after scaling/convergence for both the simulation and data processing

Validation of the η estimate from the constrained fit

- From the constrained fit we obtain η = 0.1958 ± 11.2% statistical error
- This is systematically lower than the value estimated by using the laser parameters

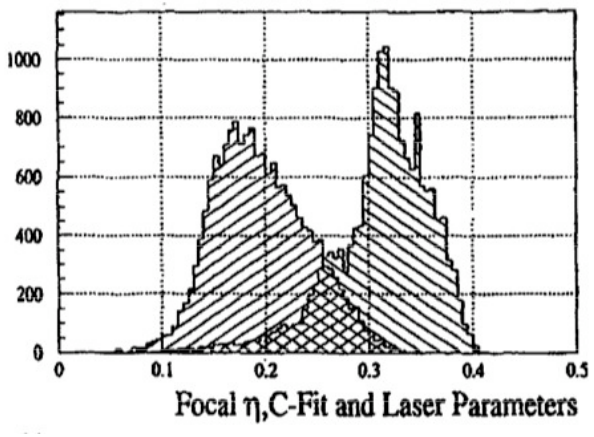

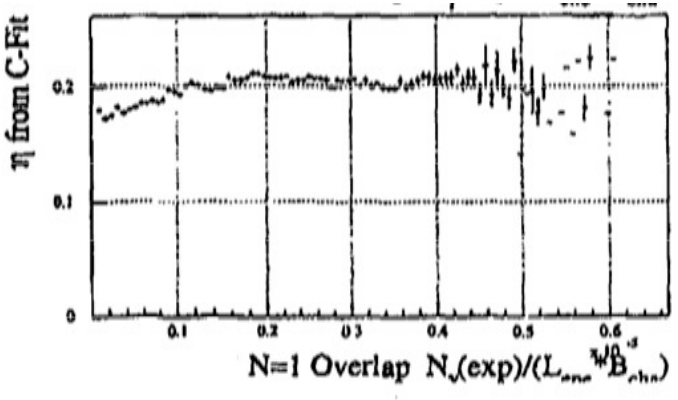

- The Compton scattered e^- rates measured by ECAL support the η values from the fit:
  - Compton scattering measurements have bee independently verified and compared to MC
- Measured η is only a function of the laser characteristics:
  - Compute the ratio of n=1 γ's normalized to laser energy and e^- per bunch
  - This ratio depends only on the laser/electron beam overlap hence independent of η
- Systematic errors on the η estimate include:
  - Contamination of the non-linear monitor signal by lower order signals
  - Contamination of all monitor signal by background electrons
  - Different signal scaling factors, due to monitor miss-calibration
  - Different signal error scaling due to monitor miss-calibration

$$\langle \eta \rangle = 0.1958 \pm 11.2\%(stat.)^{+7.97\%}_{-12.61\%}(syst.)$$

Inefficiency corrections and background estimates

- Before we compare the data to the simulation predictions some corrections are necessary:
  - Corrections due to mismatch in the timing of the laser and the electron beams
    - Amounts to ~5ps in timing offset between the two beams
  - Corrections due to mismatch in the position of the electrons and the laser beams
    - Amounts to ~25μm jitter in the x-position
    - Negligible in the case of the y-position
  - Corrections due to the inefficiency of the e^+ cluster search algorithm
    - Embed simulated positrons into background using real data (both laser ON and OFF triggers)
    - Run the e^+ cluster search algorithm and count the efficiency of finding those
    - Resultant inefficiency of ~7%
- An estimate of the residual background is also necessary:
  - Need to establish the fact that the e^+ rate is above the residual background
  - Origin of the residual background are e^+ from showers of lost particles on the beam pipe
  - Calculate the 95% confidence level assuming a Poisson distribution for the background
  - Background contribution significant for data taken at low laser intensity η values
  - Signal well above residual background at high η values

49.1 GeV electron beam data analysis main differences

- The 49.1 GeV data analysis proceeds along the same lines with the 46.6 GeV one
- One major difference is the higher residual background levels:
  - Electron beam tuning more demanding when moving to higher energies
  - Only the later runs are kept for further analysis
  - Significantly more limited statistics

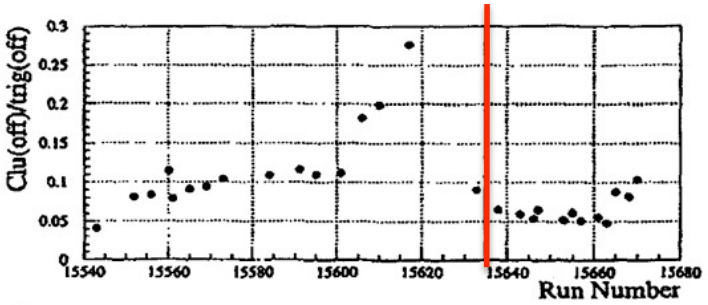

Analyzed runs above the red vertical line

- Use the electron calorimeter (ECAL) to estimate η in addition to the constrained fit:
  - Problems of the non-linear monitors during some of the useful 49.1 GeV runs
  - Severely affects the validity of the constrained fit results in this case
  - ECAL signal also η dependent, can be used to extract η value from measured electron rates

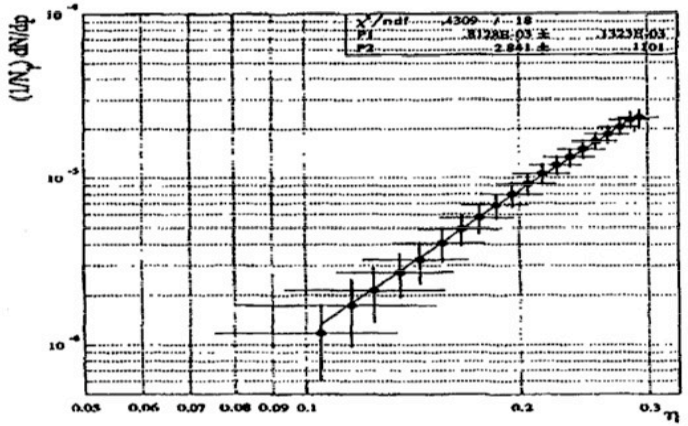

Relation of measured electron rates by ECAL as a function of the laser intensity η. Used as an alternative to estimate η for some of the 49.1 GeV data. A 10% systematic error on η is introduced.

$$\langle \eta \rangle = 0.2183 \pm 9.2\%(stat.)^{+5.35\%}_{-14.02\%}(syst.)$$

Multi-photon Pair Production Results

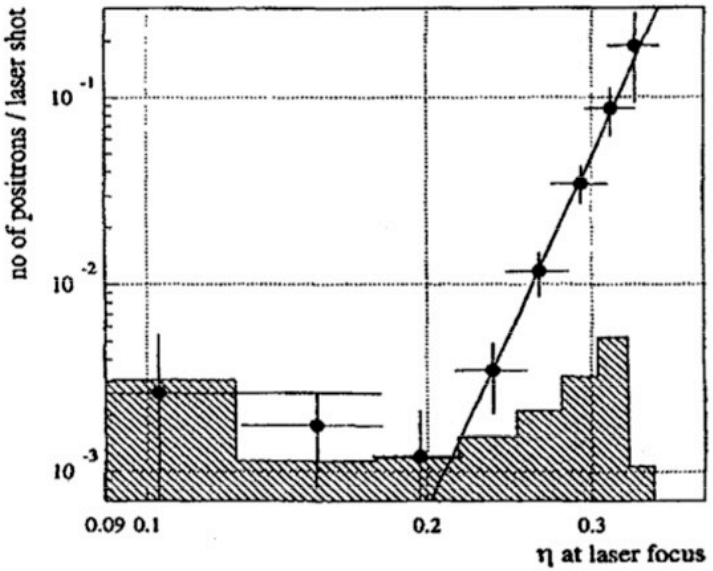

Total signal is 106 ± 14 positrons

Perform a power law fit. Slope indicative of the number of photons participating

$$n = 5.1 \pm 0.2\ (\text{stat.})\ ^{+0.5}_{-0.8}\ (\text{syst.})$$

Low η region compatible with residual background from beam showering. Concentrate on events with η>0.

Measured positron spectrum in good agreement with MC predictions.

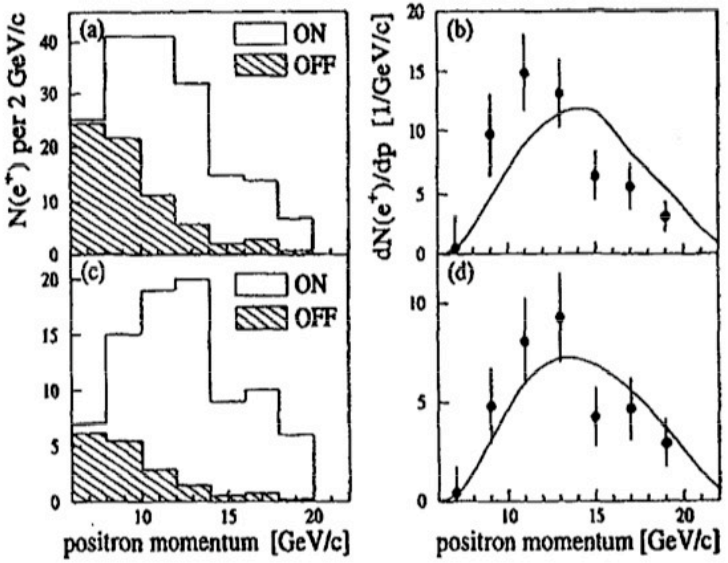

Multi-photon Pair Production Results

Another 22 ± 10 positrons have been accumulated at 49.1 GeV electron energy.

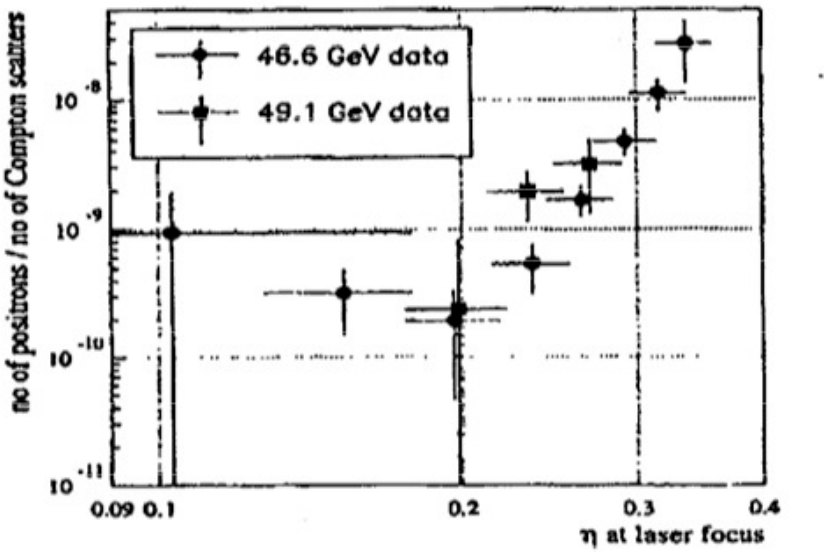

Putting them together with the 46.6 GeV data we see that the positron production rate increases by a factor of 2-3 as expected from the theoretical predictions

Spontaneous Vacuum Breakdown Results

- The pair production rates can be plotted as a function of 1/Y
- In this case they should follow an exponential law
- This will be a manifestation of the spontaneous vacuum breakdown
- The dependence on 1/ should be independent of the electron beam energy

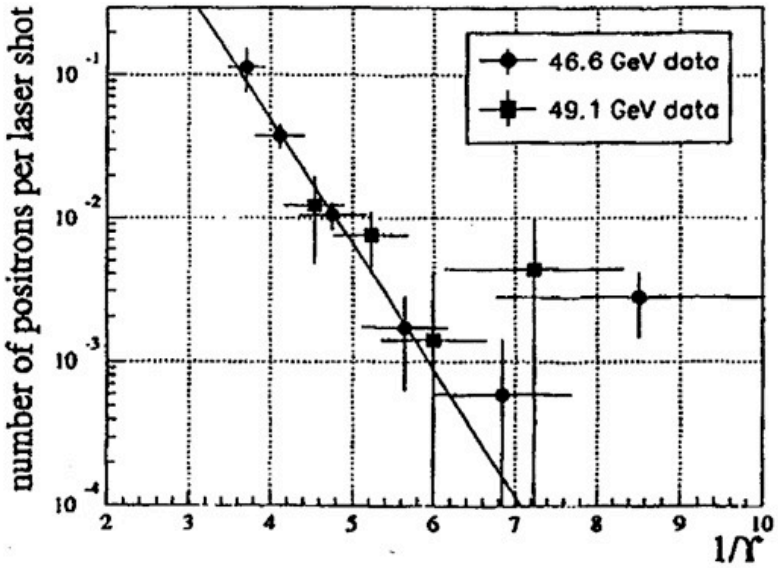

Fitting an exponential one then obtains:

$$\pi g(1/\eta) = 1.78 \pm 0.11\ (\text{stat.})\ {}^{+0.18}_{-0.53}\ (\text{syst.})$$

Compare to 1.93 predicted by theory

Summary and Conclusions

- The production of e^+e^- pairs during the scattering of an intense laser beam off a high energy electron beam has been observed experimentally
- The data can be successfully interpreted in two ways:
  - As a demonstration of the multi-photon Breit-Wheeler process within the regime of the non-linear QED
  - As the observation of "sparking" of the vacuum, within the context of vacuum polarization
- Semi-classical theoretical models describing non-linear QED effects have for the first time been tested experimentally. They were found to agree well with the measurements
- A new area of experimental research has been pioneered
  - Laser pulse-widths of ~1 ps have for the first time been produced and led to further improvements in the field of laser technology
  - Techniques developed for the timing of short beams have been widely employed since
  - The produced high energy γ's with their small angular diversion (few μ-radians) have demonstrated a possible method for the production of a γ beam in future linear collider
  - A number of theoretical and experimental endeavors have sprung up since the conclusion of E-144
  - The field of strong-field and non-linear effects physics has been flourishing closely following the developments in laser technology
- The experiment itself and in particular the pair production results have received wide publicity over time. One can refer to the site www.slac.stanford.edu/exp/e144/popular.html